Available online at www.sciencedirect.com
ScienceDirect
Geochimica et Cosmochimica Acta 72 (2008) 6069–6078
Geochimica et Cosmochimica Acta
www.elsevier.com/locate/gca

Stability of biomass-derived black carbon in soils

Biqing Liang [a], Johannes Lehmann [a,*], Dawit Solomon [a], Saran Sohi [b], Janice E. Thies [a], Jan O. Skjemstad [c], Flavio J. Luizão [d], Mark H. Engelhard [e], Eduardo G. Neves [f], Sue Wirick [g]

[a] *Department of Crop and Soil Sciences, College of Agriculture and Life Sciences, Cornell University, 909 Bradfield Hall, Ithaca, NY 14853, USA*
[b] *Department of Soil Science, Rothamsted Research, Harpenden AL5 2JQ, UK*
[c] *CSIRO Land and Water, Glen Osmond, SA 5064, Australia*
[d] *Instituto Nacional de Pesquisa da Amazônia (INPA), 69011-970 Manaus, Brazil*
[e] *Environmental Molecular and Sciences Laboratory, Pacific Northwest National Laboratory, Richland, WA 99352, USA*
[f] *Museu de Arqueologia e Etnologia, Universidade de São Paulo, Sao Paulo, SP 05508-900, Brazil*
[g] *Department of Physics and Astronomy, State University of New York at Stony Brook, Stony Brook, NY, USA*

Received 29 May 2008; accepted in revised form 25 September 2008; available online 8 October 2008

Abstract

Black carbon (BC) may play an important role in the global C budget, due to its potential to act as a significant sink of atmospheric CO_2. In order to fully evaluate the influence of BC on the global C cycle, an understanding of the stability of BC is required. The biochemical stability of BC was assessed in a chronosequence of high-BC-containing Anthrosols from the central Amazon, Brazil, using a range of spectroscopic and biological methods. Results revealed that the Anthrosols had 61–80% lower ($P < 0.05$) CO_2 evolution per unit C over 532 days compared to their respective adjacent soils with low BC contents. No significant ($P > 0.05$) difference in CO_2 respiration per unit C was observed between Anthrosols with contrasting ages of BC (600–8700 years BP) and soil textures (0.3–36% clay). Similarly, the molecular composition of the core regions of micrometer-sized BC particles quantified by synchrotron-based Near-Edge X-ray Fine Structure (NEXAFS) spectroscopy coupled to Scanning Transmission X-ray Microscopy (STXM) remained similar regardless of their ages and closely resembled the spectral characteristics of fresh BC. BC decomposed extremely slowly to an extent that it was not possible to detect chemical changes between youngest and oldest samples, as also confirmed by X-ray Photoelectron Spectroscopy (XPS). Deconvolution of NEXAFS spectra revealed greater oxidation on the surfaces of BC particles with little penetration into the core of the particles. The similar C mineralization between different BC-rich soils regardless of soil texture underpins the importance of chemical recalcitrance for the stability of BC, in contrast to adjacent soils which showed the highest mineralization in the sandiest soil. However, the BC-rich Anthrosols had higher proportions (72–90%) of C in the more stable organo-mineral fraction than BC-poor adjacent soils (2–70%), suggesting some degree of physical stabilization.

1. INTRODUCTION

Black carbon (BC) includes a wide variety of fire-derived polymeric, aromatic and graphitic C forms, such as char, charcoal, soot and graphite (Goldberg, 1985; Jones et al., 1997). Black C is ubiquitous in terrestrial environments with significant amounts in some soils (Schmidt and Noack 2000; Schmidt, 2004; Preston and Schmidt, 2006). It may play an important role in the global C budget, due to its potential to act as a significant sink of C from the relatively rapid bio-atmospheric C cycle to the slower geological C cycle (Seiler and Crutzen, 1980; Kuhlbusch and Crutzen, 1996; Forbes et al., 2006).

Black C exhibits a high degree of resistance to a range of chemical oxidants (Skjemstad et al., 1996; Bird and Gröcke,

* Corresponding author. Fax: +1 607 255 3207.
E-mail address: CL273@cornell.edu (J. Lehmann).

0016-7037/$ - see front matter © 2008 Elsevier Ltd. All rights reserved.
doi:10.1016/j.gca.2008.09.028

1997). Studies using ^{14}C dating revealed that BC represented the oldest fraction of C in soils (Pessenda et al., 2001). The most resistant component was estimated to have an average turnover time in the order of several thousands of years (Preston and Schmidt, 2006; Masiello, 2004).

The great age of BC in the environment may indicate that the degradation of BC through microbial or inorganic reactions over time is negligible. However, this assumption leads to a difficulty in balancing the global BC budget. It is now widely accepted that a significant quantity of BC must have undergone degradation in terrestrial environments (Kuhlbusch, 1998; Schmidt and Noack, 2000; Druffel, 2004; Masiello, 2004; Schmidt, 2004; Forbes et al., 2006). In order to fully evaluate the influence of BC on the global C cycle, a better understanding of the degradation of BC in soils is required, which would allow uncertainties and discrepancies regarding estimates of BC fluxes between the atmosphere, biosphere and oceans to be minimized.

Photochemical abiotic oxidation and microbial decomposition were suggested as the two major mechanisms for BC degradation (Goldberg, 1985). Bird and Cali (1998) concluded that charred organic matter slowly degrades and at least some components of BC are very long lived (Forbes et al., 2006). The stability and resistance of BC against biotic and abiotic oxidation is highly variable due to various sources of original materials, production procedures and temperatures (Nishimiya et al., 1998; Schmidt and Noack, 2000; Baldock and Smernik, 2002; Masiello, 2004; Kawamoto et al., 2005). Contradictory experimental results reported both rapid (Bird et al., 1999) and slow (Shindo, 1991) decomposition of biomass-derived BC in soils. The pattern of BC oxidation in soils remains to be resolved, and little is known about the interaction between BC surfaces and clay minerals (Brodowski et al., 2006; Liang et al., 2006). Quantifying to what extent oxidation occurs on the surfaces of BC particles (Cheng et al., 2006) will provide important information about the processes influencing BC disappearance (Lehmann et al., 2005).

Therefore, we examined the changes of BC stability and its molecular composition over millennial time scales in soils, by using a 'chronosequence' of ancient BC-rich Anthrosols (Terra Preta de Indio) and their adjacent soils from the central Amazon, Brazil.

2. MATERIALS AND METHODS

2.1. Sites and soil sampling

Black C-rich Anthrosols and low-BC adjacent soils with identical mineralogy (Liang et al., 2006) were sampled from four sites, Hatahara (HAT), Lago Grande (LG), Açutuba (ACU) and Dona Stella (DS), near Manaus, Brazil (3°8′S, 59°52′W, 40–50 m above the sea level) (Table 1). The Anthrosols (locally known as 'Terra Preta de Indio') are the result of pre-Columbian settlements, developed on Oxisols, Ultisols, or Spodosols. Lago Grande was covered by an old secondary forest, whereas HAT and ACU showed signs of recent agricultural activities, and DS was under natural *campinarana* vegetation. The period of occupation and therefore the age of the BC at each site has been estimated to range from 600–1000 years BP at HAT, to 900–1100 at LG, 2000–2300 at ACU to 6700–8700 years BP at DS (Neves et al., 2003; Liang et al., 2006). Adjacent soils were chosen on the basis of maximum color difference compared to the BC-rich and dark Anthrosols which consistently contain artifacts, selecting those of typically pale yellow or white soil color, and with no visible signs of human activities. Samples were taken from soil profiles at various depths according to horizons (Table 1) containing distinct depositional features, after removal of the litter layer if present. The analyses of BC properties were done only for one horizon per soil type and site due to time-demanding spectroscopic measurements. Subsoil horizons were taken in some cases to exclude any recent BC inputs. The depths of the BC enrichment varies due to its anthropogenic origin. Analyses of adjacent soils were done for the A horizon. All samples were air-dried and large plant debris was removed. Detailed soil properties were included in Liang et al. (2006).

2.2. Nuclear magnetic resonance spectroscopy (NMR) and BC content

To estimate the BC contents of the soil samples, the functional group chemistry of all organic C was assessed by applying ^{13}C Nuclear Magnetic Resonance (NMR) spectroscopy with cross polarization / magic angle spinning (CP/MAS) after pre-treatment with HF (2% wt/vol) for both high-BC Anthrosols and adjacent soils from four sites

Table 1
Properties of BC-rich Anthrosols and adjacent soils in the central Amazon.

Site	Type	Depth (cm)	Age (years BP)	pH		Organic C (mg g^{-1})	Total N (mg g^{-1})	C/N ratio	Sand (%)	Silt	Clay
				1:2.5 (H_2O)	1:2.5 (KCl)						
HAT	Anthrosol	43–69	500–1000	6.4	5.5	22.0	1.0	23	51.3	21.7	27.0
	Adjacent soil	0–10		4.6	3.8	21.8	1.6	14	60.4	3.8	35.9
LG	Anthrosol	0–16	900–1100	5.9	4.9	31.5	1.8	18	47.9	29.6	22.6
	Adjacent soil	0–8		4.2	3.5	17.5	1.3	14	69.4	3.9	26.7
ACU	Anthrosol	48–83	2500–3000	5.6	4.2	15.7	1.0	16	81.9	7.7	10.4
	Adjacent soil	0–30		4.7	3.9	15.4	0.8	20	87.9	3.6	8.5
DS	Anthrosol	Buried (190–210)	6700–7000	5.0	4.1	16.5	1.1	15	96.8	2.9	0.3
	Adjacent soil	0–12		3.9	2.6	10.2	0.4	27	91.1	8.6	0.3

(HAT, LG, ACU, and DS) according to Skjemstad et al. (1999). Seven peak regions were assigned, namely alkyl C (0–45 ppm), *n*-alkyl/methoxyl C (45–60 ppm), *O*-alkyl C (60–95 ppm), Di-*O*-alkyl C (95–110 ppm), aromatic C (110–145 ppm), phenolic C (145–165 ppm) and amide/carboxyl C (165–215 ppm). The total peak area within each region was integrated and the contribution of each functional group to total C was expressed as a percentage of the total. The BC (char) contents were obtained using a molecular mixing model developed by Nelson and Baldock (2005). Since the CP/MAS technique can greatly underestimate the aryl C present in chars by as much as 50% when compared to a less discriminatory but impractical Bloch Decay approach (BD/MAS) (Skjemstad et al., 1996), the final BC contents were reported using a correction factor of 0.27 for CP observability (Skjemstad et al., 1999).

2.3. Incubation and C mineralization

A long-term incubation experiment over 532 days was used to measure C mineralization in both high-BC Anthrosols and low-BC adjacent soils from three sites (HAT, ACU and DS which presented the largest spread in BC ages). One hundred grams of soil was added to 0.95-L wide-mouth and airtight Mason jars, and incubated under a constant temperature of 30 °C. The jars were arranged in a randomized complete block design (RCBD) with four replicates. Soil moisture contents were adjusted to 55% of field capacity before the incubation started and maintained throughout the experiment using repeated weighing. The field capacity was determined gravimetrically.

Between 0.2 and 1.0 g of soda lime (Mallinckrodt Baker, Paris, KY, highest absorption capacity 26%) were placed in 30-mL Qorpak vials as sorbent, which were dried for 24 h at 105 °C before and after incubation. Evolved CO_2 from C mineralization was trapped by the soda lime and mineralized C was quantified gravimetrically with a conversion factor of [1.69 × (weight gain) × 12/44] (Edwards, 1982; Grogan, 1998). The amount of CO_2 evolved is proportional to the weight increase in soda lime dry mass (Grogan, 1998). The incubation experiment was run for 532 days with 14 times of sampling after 1, 2, 8, 18, 38, 65, 92, 128, 177, 236, 305, 366, 456 and 532 days.

Curve fitting using a double-exponential model (Sigmaplot 2000, tolerance $1e^{-10}$, stepsize 100, and iterations 1200–2500) was performed to mathematically define the size and turnover rate of two source pools, conceptually corresponding to (i) a large stable pool with a slow turnover rate comprising BC and/or stable SOM and (ii) a smaller and easily mineralizable C pool of higher turnover rate which is also called labile pool. The equation used to fit cumulative CO_2 evolution was:

$$X_t = X_1\left(1 - e^{-k_1 t}\right) + X_2\left(1 - e^{-k_2 t}\right)$$

Where X_t = mineralizable C; X_1 = size of the labile C pool; X_2 = size of the stable C pool; k_1 and k_2 = mineralization rates of the labile and stable pools, respectively; and t = time of incubation (days). We compared the cumulative respiration from BC-rich Anthrosols and BC-poor adjacent soils. Values were normalized per unit soil C for evaluating the C mineralization capacity or stability. The unit for X_t, X_1 and X_2 is mg CO_2–C g^{-1} C.

2.4. NEXAFS spectroscopy and C functional group chemistry

Synchrotron-based Scanning Transmission X-ray Microscopy (STXM) coupled with Near-Edge X-ray Absorption Fine Structure (NEXAFS) spectroscopy was used to map the spatial distribution of C forms on BC particle thin sections with a resolution of 50 nm (Lehmann et al., 2005). Spectroscopic measurements were done on BC particles isolated from four Anthrosol soils (HAT, LG, ACU and DS). Ultra-thin sections of 200–400 nm thickness were prepared using an ultra-microtome (Ultracut UTC, Leica Microsystems Inc., Bannockburn, IL) with a diamond knife (MS9858 Ultra 45°, Diatome Ltd., Biel, Switzerland) after being embedded in supercooled elemental sulfur (see Lehmann et al., 2005, for details). Images were recorded below and above the K-edge (attenuation coefficient of photons just above the binding energy of the K shell electron of the atoms interacting with the photons) of C (284.3 eV for absorption) at the X-1A1 end-station of the National Synchrotron Light Source at Brookhaven National Laboratory (Upton, NY). Images taken at different energy levels were stacked and analyzed according to methods described by Lehmann et al. (2005) and Liang et al. (2006). After principal component and cluster analyses (PCA_GUI 1.0, Lerotic et al., 2004) were done to classify sample regions with similar spectral characteristics on orthogonalized and noise-filtered spectra, target maps (representing similar spectra and chemical composition) and associated target spectra were obtained by singular value decomposition (SVD) (Lehmann et al., 2005). The target maps and corresponding spectra for the studied BC samples were presented in Liang et al. (2006) and showed clear patterns of greater oxidation near the surfaces of BC particles than in the interior regions. According to their spectral and morphological properties, BC could be distinguished from adsorbed non-BC (Liang et al., 2006). This study quantifies the C functional groups by spectral deconvolution of the different regions within the BC particles from HAT, LG, ACU and DS sites, fresh BC and humic substances. We compared the molecular composition of the interior of the BC particles, which comprised the majority of the BC area, for different ages of BC ranging from 600 to 8700 years.

The deconvolution and curve fitting of the different C functional groups was performed using the Extended X-ray Absorption Fine Structure (EXAFS) analysis software Athena 0.8.052 (Ravel and Newville, 2005). A 'G-9' deconvolution scheme (G represents fitting with Gaussian functions) with eight diagnostic bands was adopted, which was different from the 'G-7' scheme with five major C 1-s peaks proposed by Scheinost et al. (2001) and Schumacher (2005), or the 'G-9' scheme with seven diagnostic bands used by Solomon et al. (2005). We developed this deconvolution scheme for BC samples in response to our findings that an additional peak at 286.1 eV is characteristic for BC particles (Liang et al., 2006), which was not identified as an important spectral feature in previous studies that

have focused on humic substances. One arctangent function was fixed at 290 eV with a full width at half maximum (FWHM) of 1.0 eV (Schumacher et al., 2005) for modeling the ionization step. Eight diagnostic peaks were fitted with Gaussian functions at 284.3 ± 0.1 (quinone C), 285.1 ± 0.2 (aromatic C), 286.1 ± 0.1 (unsaturated aromatic C), 286.5 ± 0.2 (phenol C), 287.7 ± 0.2 (ketone carbonyl and aliphatic C), 288.5 ± 0.3 (carboxyl C), 289.3 ± 0.2 (carbonyl C) and 290.6 ± 0.2 (carbonate C) eV for electronic transitions. The sum of the peak areas from eight Gaussian peaks and the area of the arctangent function 290 eV was set to 100%. The peak area of each electronic transition was transformed into percentages of the sum of all functional groups. Quinone C, aromatic C and unsaturated aromatic C were grouped together to represent the un-oxidized fraction of BC, which contains mainly stable C═C bonds. Ketone carbonyl C, carboxyl C and carbonyl C were combined as the oxidized C fractions. Spectral deconvolution was reported for two sections from each site (HAT, LG, ACU and DS), which were obtained from different BC particles and labeled as BC-1 and BC-2. The cross section of BC particles showed a three-layer pattern of progressive oxidation from surface to the core with distinct spectral characteristics, which were distinguished as interior, intermediate and outer region.

2.5. X-ray photoelectron spectroscopy and BC aromaticity

X-ray Photoelectron Spectroscopy (XPS) is capable of quantifying surface properties (especially surface functional groups), by probing a maximum depth of about 10 nm on a solid sample surface (Cheng et al., 2006). Whole scanning and detailed carbon (C 1s) high-resolution scanning were used to quantify functional groups either (i) on BC surfaces by measuring intact BC particles, or (ii) within entire particles by grinding BC prior to measurement. Black C particles were carefully isolated under a light microscope, and mounted on a standard XPS sample holder. Each XPS measurement was a composite analysis of over 100 BC particles. XPS measurements were conducted at the Wiley Environmental Molecular Sciences Laboratory using a physical electronic quantum 2000 scanning ESCA Microprobe (Physical Electronics GmbH, Ismaning, Germany), coupled with a focused monochromatic Al Kα X-ray (1486.7 eV) source for excitation and a spherical section analyzer.

XPS spectra were analyzed and deconvoluted with a non-linear least squares curve fitting program (XPSPEAK 4.1, by R. Kwok, CUHK). A Shirley background correction was done on regions from 280 to 295 eV.

The C 1s binding energy of aromatic C (aromatic CH C1s) was assigned at 284.6 eV. And a shift of 1.6 (±0.2), 3.0 (±0.2) and 4.5 (±0.1) eV above 284.6 eV was defined as C—O, C═O and COO, respectively (Proctor and Sherwood, 1982; Cheng et al., 2006). For a valid comparison, identical Full-Width Half-Maximum (FWHM) values were used, with a value of 1.94, 1.52, 1.62 and 1.78 for peaks at 284.6, 286.2, 287.6 and 289.1 eV, respectively. No fixed FWHM values were used for spectra of BC particles from the DS site. The adopted values of FWHM were derived from measurements of 53 samples, among which only a limited number of samples are reported in this study. The Gaussian–Lorentian ratios were freely fit for all different peaks in this study.

2.6. Soil fractionation and C stabilization within soil components

Apart from studying the chemical and biological stability of BC, the association of BC with aggregates and minerals was investigated using a density fractionation method to determine to what extent BC was protected by either soil aggregation or possible formation of organo-mineral interactions for samples from HAT, ACU and DS sites. Three organic matter fractions (free light, intra-aggregate light and organo-mineral) were sequentially separated from Anthrosols and adjacent soils, which were not incubated, using a combination of a density agent (NaI) and physical disruption according to the method described by Sohi et al. (2001). Briefly, 15 g of re-wetted soil (at least two replicates) were added to 0.09 L sodium iodide (NaI) solution with a density of 1.800 (±0.025) mg m^{-3} in a 0.25-L polycarbonate centrifuge bottle. The soil was suspended, swirled for 30 s to break down unstable aggregate and centrifuged at 8000 *g* for 30 min to separate the floating light fraction and heavy particles. This 'free' light fraction was isolated by vacuum filtering (Millipore) onto a glass fiber filter (Type GF/A, 47 mm diameter, 1.6 μm retention; Whatman), rinsed thoroughly with deionized water to remove soil mineral and salt contaminants and transferred to a separate collector. An intra-aggregate light fraction was then isolated from stable aggregates in the remaining soil by re-adding the NaI solution to the bottle, re-suspending the remaining soil material, and sonicating (Misonix XL 2020, Farmingdale, NY) for 200 s with a 19-mm diameter probe and a submersion depth of 19 mm. Actual sonication energy was determined to be 0.75 kJ g^{-1} soil. The intra-aggregate light fraction was separated using the same procedure described for the free light fraction. Lastly, the residual organo-mineral fraction was recovered from the bottles, and dried after removal of excess NaI salt by repeated addition of deionized water and centrifugation (8000×*g*, 15 min).

The C contents of each fraction and original soil samples were determined using a Europa ANCA 20/20 CN analyzer (PDZ Europa Ltd., Crewe, UK). The C amounts associated with each fraction were calculated by multiplying the C content (mg kg^{-1} soil) of each fraction by their respective dry weights.

2.7. Statistics

Analysis of variance (ANOVA) was performed with the SAS program (SAS Institute Inc., Cary, NC) to determine the significance of differences between CO_2 evolved from different Anthrosols and adjacent soils. Multiple comparisons of means for significant main effects were conducted using least significant difference (LSD) at $P < 0.05$, unless otherwise indicated.

3. RESULTS

3.1. Black C contents

The aromaticity of organic C in Anthrosols and adjacent soils was measured by (CP/MAS) ^{13}C NMR, and calculated based on the percentage of aromatic C to total C (Table 2). Anthrosols had 42% (HAT), 30% (LG), 33% (ACU) and 36% (DS) of aromatic C, which were 76%, 81%, 24% and 66% higher than in their adjacent soils, respectively (Table 2). At the same time, Anthrosols also contained 17% (HAT), 16% (LG), 21% (ACU) and 17% (DS) more carboxylic C compared to the adjacent soils. The estimated BC content was 293% (HAT), 555% (LG), 65% (ACU) and 608% (DS) higher in the Anthrosols than that in the adjacent soils.

3.2. Carbon mineralization

The highest CO_2 evolution per unit SOC was observed on the first day after the incubation started. The adjacent soil from HAT (8.3 mg CO_2–C g^{-1} C day^{-1}) had the highest CO_2 evolution, which was followed by DS (7.4 mg CO_2–C g^{-1} C day^{-1}) and ACU (6.1 mg CO_2–C g^{-1} C day^{-1}). The Anthrosol from HAT had the highest CO_2 evolution (2.9 mg CO_2–C g^{-1} C day^{-1}) within the three Anthrosol sites. CO_2 evolution decreased sharply after the first 2 days and reached equilibrium of lower CO_2 evolution after the first week for both Anthrosols and adjacent soils at all sites (Electronic annex Table 1).

During the incubation, high-BC-containing Anthrosols were consistently found to have significantly ($P < 0.05$) lower CO_2 evolution per unit soil C, compared to the corresponding adjacent soils at each sampling point, and 61–80% lower total evolution per unit SOC at the end of 532 days of incubation (Fig. 1). The labile C pool obtained by curve fitting was 27.0%, 19.8% and 24.7% of the total SOC and contributed 29.9%, 19.9% and 10.3% to the total mineralizable C in HAT, ACU and DS adjacent soils, respectively (Table 3). In contrast, only 9.0%, 6.0% and 6.7% of the total SOC resided in the calculated labile C pool in the BC-rich Anthrosols, respectively. At the ACU site, the size of the stable pool in the Anthrosol is around three times of that in the adjacent soil and the proportion of the stable C pool in the Anthrosol was 21.4% greater than that in the adjacent soil. The kinetic loss constant (k_2) of the stable C pool in the Anthrosol was one order of magnitude lower than that in adjacent soils (Table 3). It should be noted that the fit for the stable pool of the Anthrosols is poor presumably due to its high stability that was imperfectly captured during the incubation period, and results for the stable pool have to be viewed with caution.

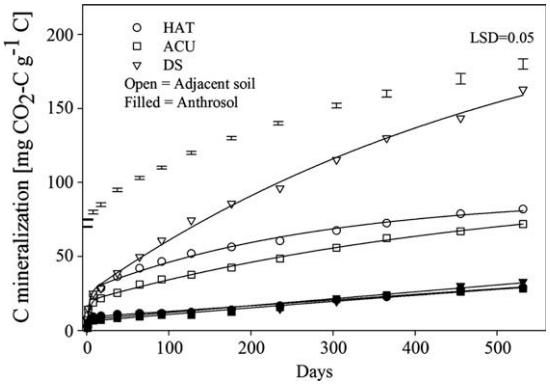

Fig. 1. Cumulative C mineralization per unit soil C in Anthrosols and adjacent soils from site HAT, ACU, DS in a long-term incubation experiment (532 days, means and standard errors, $N = 4$, LSD = least significant difference between all treatments within one time point at $P < 0.05$; curves fitted by using a double-exponential equation with parameters shown in Table 3).

After 532 days, 16.3%, 8.2% and 7.2% of the total SOC in adjacent soils were respired as CO_2 in the DS, HAT and ACU sites, respectively (Fig. 1), which were equivalent to about 30% of the entire labile C pool. The proportion of mineralized C was significantly lower ($P < 0.05$) in the BC-rich Anthrosols, with only 3.3%, 2.9% and 2.8% in DS, HAT and ACU, respectively. The turnover time of total SOC (calculated as the ratio of soil C and CO_2–C loss over 532 days at the 30 °C incubation temperature) was 9, 18 and 20 years in adjacent soils, but 44, 50 and 52 years in BC-rich Anthrosols for DS, HAT and ACU sites, respectively.

3.3. Molecular properties of BC using NEXAFS

Deconvolution of NEXAFS spectra established the contribution of each C functional group as a percentage of total C. A large and well defined peak was found near

Table 2
Carbon functional groups obtained by NMR spectroscopy and BC contents of the studied soils estimated by a molecular mixing model.

Site	Alkyl (0–45) (ppm)	*N*-Alkyl / methoxyl (45–60) (ppm)	*O*-Alkyl (60–95) (ppm)	Di-*O*-alkyl (95–110) (ppm)	Aromatic (110–145) (ppm)	Phenolic (145–165) (ppm)	Amide /carboxyl (165–215) (ppm)	BC fraction (% of total C)	BC content (mg g^{-1})
HAT Anthrosol	12.7	4.1	12.5	4.5	41.5	9.5	15.2	79.4	17.5
HAT Adjacent soil	19.7	6.7	21.8	6.5	23.6	8.6	13.1	20.2	4.4
LG Anthrosol	17.8	7.3	20.5	5.9	29.6	7.0	11.9	60.9	19.2
LG Adjacent soil	22.4	8.8	27.7	7.8	16.3	6.8	10.3	9.3	1.6
ACU Anthrosol	14.9	6.0	15.6	5.6	32.6	9.7	15.7	73.1	11.5
ACU Adjacent soil	19.0	6.6	20.4	6.1	26.3	8.6	12.9	44.3	6.8
DS Anthrosol	15.6	5.9	13.6	5.4	35.5	9.4	14.7	75.1	12.4
DS Adjacent soil	21.3	7.2	22.3	6.3	21.3	9.1	12.5	10.6	1.1

Table 3
Pool sizes and decay rates of soil C mineralization using a double-exponential model.

Site	Soil type	X_1 (mg CO_2-C g^{-1} C)	X_2 (mg CO_2–C g^{-1} C)	$X_1 + X_2$ (mg CO_2–C g^{-1} C)	k_1 (day^{-1})	k_2 (day^{-1})	X_1 (% $X_1 + X_2$)	R^2
HAT	Adjacent soil	27.0	63	90	0.31	3.6E−03	29.9	0.9947
ACU	Adjacent soil	19.8	80	99.8	0.32	2.0E−03	19.9	0.9981
DS	Adjacent soil	24.7	220	244.7	0.36	1.8E−03	10.3	0.9971
HAT	Anthrosol	9.0	1.6E+06	1.6E+06	0.41	2.4E−08	0.0	0.9940
ACU	Anthrosol	6.0	2.1E+02	2.2E+02	0.42	2.1E−04	2.7	0.9876
DS	Anthrosol	6.7	4.4E+06	4.4E+06	0.40	1.1E−08	0.0	0.9749

X_1 and X_2 = size of the labile and stable C pools.
k_1 and k_2 = mineralization kinetic constants/rates of the labile and stable C pools.

285.0 eV for all BC samples, which can be unambiguously assigned to double carbon–carbon (C═C) bonds without hetero-atoms as nearest neighbors (Stöhr, 1996). A peak at 287.7 (±0.1) eV most likely represents ketone carbonyl (Braun et al., 2005; Haberstroh et al., 2006), though a weak 1s–3p/σ^* symmetrical antibonding C─H* can also be assigned (Schäfer et al., 2005). A FWHM of 0.6 eV (±0.1) was found most appropriate for all the bands in most samples, except quinone C and carboxylic C, for which 0.4 eV was used.

NEXAFS analyses showed that 22.7% (LG BC-1) to 31.8% (ACU BC-1) of the interior regions of BC particles remained in un-oxidized C forms, only slightly lower than that of fresh BC (32.7%) (Table 4). These values were about two times higher than those in humic substances. The interior region of the BC particles showed a consistently higher un-oxidized fraction (22.7–31.8%) than the intermediate (21.3–30.0%) and outer regions (17.4–29.8%). The ratio of un-oxidized to oxidized organic C also consistently showed a decrease from the interior region to the particle surfaces (Table 4). No systematic change was observed for un-oxidized C of the interior regions of BC samples between sites of different BC ages (600–8700 years), clearly showing that the un-oxidized fraction of the BC interior region remained similar over long periods of time and closely resembled the spectral characteristics of fresh charcoal BC (Fig. 2 and Table 4).

Table 4
Carbon forms determined by NEXAFS spectral deconvolution of the different spatial regions within BC particles from different Anthrosols, in comparison to charcoal BC and two humic substances extracts.

Site	Region in particle	Un-oxidized C (%)	Oxidized C (%)	Un-oxidized to oxidized C (ratio)
HAT BC-1	Interior	30.6	31.5	1.0
	Intermediate	29.2	32.2	0.9
	Outer	26.5	34.2	0.8
HAT BC-2	Interior	28.6	33.7	0.9
	Intermediate	24.2	34.0	0.7
	Outer	23.8	37.0	0.6
LG BC-1	Interior	22.7	34.8	0.7
	Intermediate	21.3	34.6	0.6
	Outer	21.3	34.1	0.6
LG BC-2	Interior	26.9	33.9	0.8
	Intermediate	26.9	36.5	0.7
	Outer	25.3	35.2	0.7
ACU BC-1	Interior	31.8	33.6	1.0
	Intermediate	30.0	31.8	0.9
	Outer	29.8	32.1	0.9
ACU BC-2	Interior	24.3	33.9	0.7
	Intermediate	21.5	35.8	0.6
	Outer	17.4	42.9	0.4
DS BC-1	Interior	28.6	34.8	0.8
	Outer	25.8	35.8	0.7
Charcoal		32.7	33.4	1.0
Hu. HA		12.6	41.1	0.3
Hu. LG		10.3	42.5	0.2

BC-1 and BC-2 represent sections from two different BC particles.
Hu. HA = humic substance from HAT.
Hu. LG = humic substance from LG.

3.4. Molecular properties of BC using X-ray photoelectron spectroscopy

Deconvolution was performed on high-resolution XPS spectra of C 1s to quantify different C forms. Up to 54.5–61.3% and 60.3–62.1% of the C was found in aromatic C form on BC particle surfaces and entire particles (Table 5), respectively. No obvious correlation between the percentages of aromatic C forms and the ages of BC from different sites was observed (Fig. 2). Thus the stability of BC (reflected by the portion of aromatic C) remained similar over time, which confirmed the result of the NEXAFS analyses. The Si and Al contents also remained in the same order of magnitude between sites with slightly higher contents on BC surfaces and lower contents in the sandy DS soil (Table 5). In contrast, the carboxyl functional groups (COO) increased over time, associated with a decrease in C—O groups.

3.5. Carbon in different soil fractions

Based on Sohi et al. (2001), we considered the free light fraction to be the relatively labile pool, the intra-aggregate light fraction to be the stable aggregate pool, and the organo-mineral fraction to be the most stable C pool. Anthrosols had lower soluble, free light and intra-aggregate light C than BC-poor adjacent soils. Accordingly, Anthrosols had much higher proportions (72–90%) of C in the organo-mineral fraction than adjacent soils (2–70%) (Fig. 3).

4. DISCUSSION

4.1. Stability of black carbon

A lower mineralization of organic C in similar BC-rich Anthrosols from the Amazon than in the adjacent soils has also been found by Glaser (1999). The Anthrosol soils had higher pH, higher base cation and P contents as compared to the adjacent soils (Liang et al., 2006), which typically increases decomposition as shown for soils with different pH values (Waschkies and Hüttl, 1999). Thus the higher stability of organic C against microbial decomposition is a result of the high BC contents of these soils.

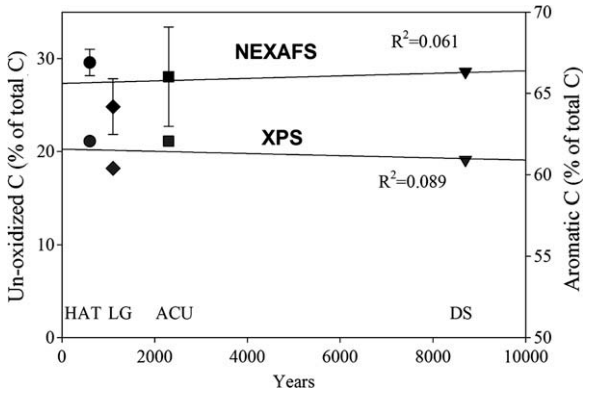

Fig. 2. Aromatic C forms of BC particles along a chronosequence over millennial time scales: un-oxidized BC (sum of quinone C, aromatic C and unsaturated aromatic C) determined by NEXAFS for interior regions of BC particles (black symbols; $N = 2$; $P < 0.05$), and aromatic C quantified by XPS for ground BC particles (dark gray symbols; $N = 1$ from a composite analysis of over 100 BC particles; $P < 0.05$).

The pool sizes of the stable C obtained by curve fitting using the double-exponential model were unrealistic large for the BC-rich Anthrosols at HAT and DS, which implied that the studied Anthrosols might operate mechanistically in a quite different manner than BC-poor adjacent soils. Inclusion of an additional pool may be needed for high-BC soils, which can not be obtained using curve fitting to the current data set, as the inclusion of a third exponential term would over-parameterize the data set. Our incubation was also likely not long enough to capture the long-term decomposition dynamics of BC in soils. While C mineralization from incubation studies can typically not be used to infer mean residence times of C under natural conditions, a comparison between the magnitude of decomposition between BC-rich Anthrosols (with 61–79% BC) and BC-poor adjacent soils (with 9–20% BC) is useful to obtain an estimate for mineralization of aged BC in soils. Decay rates (k_2) were at least one order of magnitude lower in Anthrosols than adjacent soils. Given that turnover times of soil organic matter are typically in the order of decades to 1000 years (Trumbore, 2000), the turnover time of the approximately 500- to 8000-year-old BC studied here would calculate to several centuries to several millennia.

Interestingly, the stability of the BC appeared to be similar whether the BC was only a few hundred years old or whether it was several thousand years old. This conclusion was not only evident from the mineralization experiment but also from the spectroscopic data obtained by NEXAFS and XPS. A very similar conclusion was reached by Cheng et al. (2008) who found no increase in decomposition of BC with exposure to higher mean annual temperature over 130 years determined by an incubation experiment.

This observation does not mean that BC did not decompose. In fact, it is undisputed that BC decomposes (Goldberg, 1985; Schmidt and Noack, 2000). It rather indicates that the remaining BC had the same stability regardless of age of the BC. This behavior may possibly be explained by the particulate nature of BC: oxidation of BC starts on surfaces (Cheng et al., 2006) and the interior may be protected by the outer regions of the particles that surround their core (Lehmann et al., 2005). The penetration of oxidation may be limited even for very old BC particles as demonstrated by the target maps of the studied BC particles (Liang et al., 2006). In addition, other organic matter adsorbs to BC which then surrounds the particles (Lehmann et al., 2005; Liang et al., 2006) and may be mineralized first.

While the proportion of aromatic C and the decomposition rate did not appear to change with increasing age of BC, the proportion of carboxyl groups increased at the expense of C—O and C═O groups. This may hint at continued oxidation of BC surfaces over long periods of time and could explain the increasing cation exchange capacity per unit C of BC-rich Anthrosols with age, when other C was removed by peroxide (Liang et al., 2006). However, the total amount of this long-term increase was rather small

Table 5
Black C surface functional groups determined by deconvolution of XPS spectra.

Site		Aromatic CH C 1s (%) 284.6 eV	C—O (%) 286.2 eV	C=O (%) 287.6 eV	COO (%) 289.1 eV	Al2p	Si2p
HAT	BC surface	61.3	16.8	12.3	9.6	8.9	10.1
LG		58.8	20.8	12.9	7.5	8.5	8.7
ACU		54.5	21.4	14.7	9.3	8.7	8.9
DS		59.5	13.8	12.7	14.1	4.2	1.4
HAT	Ground BC	62.1	18.4	10.3	9.2	8.3	9.8
LG		60.4	19.2	11.2	9.3	7.7	7.8
ACU		62.1	17.0	10.9	10.1	7.5	8.7
DS		60.9	13.5	11.4	14.1	4.0	2.2

compared to the rapid increases observed in the first months after BC production (Cheng et al., 2006).

The size of the labile pools in the Anthrosols as determined by the incubation study was about one-third of that in the adjacent soils. This part of the labile C calculated to be of extremely transient nature with 9–34% higher k_1 values in the BC-rich Anthrosols compared to the adjacent soils. The separation of this highly labile pool by curve fitting is likely an artifact of the large and very stable BC pool. To adequately model the stable pool in BC-rich soils may require the separation of a third pool and longer incubation.

4.2. Stabilization of black carbon

The data in this study suggest that both chemical recalcitrance as well as interactions with the mineral matrix may contribute to the stability of BC in the studied soils. It was not possible to quantify the contribution of each process, although some indication exists in this dataset that chemical recalcitrance may have played a more important role as similar C mineralization occurred for different BC-rich Anthrosols regardless of soil texture. The microbial decomposition as a fraction of soil C content was similar in all three studied Anthrosols (Fig. 1), even though the oldest BC was also associated with the sandiest soil texture in DS. Expectedly, the C mineralization in adjacent soils with low BC contents was greater with a sandier texture, in contrast to the mineralization in the Anthrosols. If minerals were to play an overriding role in protecting BC from decomposition, one would expect similar effects of soil texture on decomposition rates in both Anthrosol and adjacent soils. This was not observed in our study. An inverse relationship was found between soil clay contents and metabolic quotients as an indicator of specific microbial activity by Müller and Höper (2004). Greater specific respiratory activity in coarse-textured soils was explained by an increasing availability of substrates for mineralization than in fine-textured soils (Müller and Höper, 2004), which apparently was not the case with BC-rich soils. Three mechanisms are commonly used to explain in which way higher clay contents impede organic matter mineralization: (i) small pores can physically confine microbes and make them less active (Rutherford and Juma, 1992); (ii) surface adsorption (Oades, 1988) and (iii) entrapment in small pores of microaggregates (Hassink, 1993) can physically protect non-living soil organic matter from decomposition (Wang et al., 2003). These mechanisms appear to have a lower importance for BC than for non-BC with respect to short-term decomposition as C mineralization was not controlled by soil texture for BC-rich soil in our experiment.

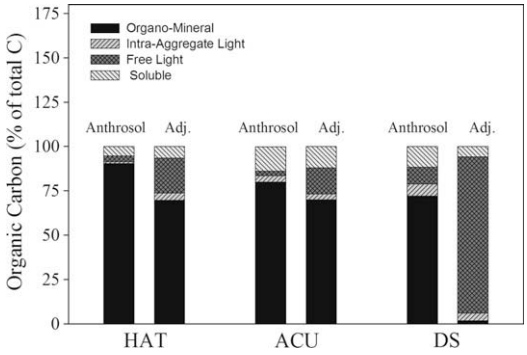

Fig. 3. Carbon distribution in each fraction as a proportion of total C of unincubated samples. Adj, Adjacent soil.

However, the distribution of C within different physical fractions was significantly different in BC-rich Anthrosols and BC-poor adjacent soils despite the almost identical total C contents, suggesting different associations between BC and minerals than observed for non-BC dominated SOC in adjacent soils. The greater amounts of C in what are commonly interpreted as more stable C pools such as the organo-mineral fraction separated by high density liquids (Baldock and Skjemstad, 1999; Baldock and Skjemstad, 2000; Falloon and Smith, 2000; Sohi et al., 2001) observed in Anthrosols than adjacent soils indicate physical protection by surficial interactions between BC and minerals. This confirms earlier reports by Brodowski et al. (2006) that BC is preferentially found within aggregates and by both Brodowski et al. (2006) and Glaser et al. (2000) that BC binds to clay minerals.

5. CONCLUSIONS

A low C mineralization indicated a lower microbial activity and lower C quality in BC-rich Anthrosols than BC-poor adjacent soils, due to the high resistance of BC to decomposition. The stability of BC appeared to remain unchanged over millennial time scales and our data suggested that chemical recalcitrance was more important than physical protection in the present dataset. However, the

contribution of these two processes to the stability of BC could not be quantified in this study. In the future, long-term controlled experiments are required to resolve this question. A challenge remains to design controlled experiments that yield information about stability over centennial and millennial time scales.

ACKNOWLEDGMENTS

This project was funded by the Division of Environmental Biology of the National Science Foundation under contract DEB-0425995. Any opinions, findings, and conclusions or recommendations expressed in this material are those of the authors and do not necessarily reflect the views of the National Science Foundation. The NEXAFS spectra were obtained at the National Synchrotron Light Source (NSLS), Brookhaven National Laboratory, a DOE supported facility at the beamline X-1A1 developed by the group of Janos Kirz and Chris Jacobsen at SUNY Stony Brook, with support from the New York State Office of Science and Technology Academic Research and NASA's Discovery Data Analysis and Exobiology programs. The XPS analyses were performed in the Environmental Molecular and Sciences Laboratory, Pacific Northwest National Laboratory, a national scientific user facility sponsored by the Department of Energy (DoE), USA. Rothamsted Research receives grant-aided support from the UK Biotechnology and Biological Sciences Research Council. Many thanks to Jeffrey A. Baldock for insightful advice, to James Kinyangi for technical discussion about NEXAFS analysis, to Helen Yates for the soil fractionation, to Fernando Costa and Manuel Arroyo-Kalin for help with sampling, and to Yuanming Zhang for invaluable help with sectioning.

APPENDIX A. SUPPLEMENTARY DATA

Supplementary data associated with this article can be found, in the online version, at doi:10.1016/j.gca.2008.09.028.

REFERENCES

Baldock J. A. and Skjemstad J. O. (1999) Soil organic carbon/soil organic matter. In *Soil Analysis–an Interpretation Manual* (eds. K. Peverill, D. Reuter and L. Sparrow). CSIRO Publishing, Melbourne, Vic., Australia, pp. 159–170.

Baldock J. A. and Skjemstad J. O. (2000) Role of the soil matrix and minerals in protecting natural organic materials against biological attack. *Org. Geochem.* **31**, 697–710.

Baldock J. A. and Smernik R. J. (2002) Chemical composition and bioavailability of thermally altered *Pinus resinosa* (Red pine) wood. *Org. Geochem.* **33**, 1093–1109.

Bird M. I. and Gröcke D. R. (1997) Determination of the abundance and carbon isotope composition of elemental carbon in sediments. *Geochim. Cosmochim. Acta* **61**, 3413–3423.

Bird M. I. and Cali J. A. (1998) A million-year record of fire in sub-Saharan Africa. *Nature* **394**, 767–769.

Bird M. I., Moyo C., Veenendaal E. M., Lloyd J. and Frost P. (1999) Stability of elemental carbon in savanna soil. *Global Biogeochem. Cycles* **13**, 923–932.

Brodowski S., John B., Flessa H. and Amelung W. (2006) Aggregate-occluded black carbon in soil. *Eur. J. Soil Sci.* **57**, 539–546.

Braun A., Huggins F. E., Shah N., Chen Y., Wirick S., Mun S. B., Jacobsen C. and Huffman G. P. (2005) Advantages of soft X-ray absorption over TEM-EELS or solid carbon studies—a comparative study on diesel soot with EELS and NEXAFS. *Carbon* **43**, 117–124.

Cheng C. H., Lehmann J., Thies J. E., Burton S. D. and Engelhard M. H. (2006) Oxidation of black carbon by biotic and abiotic processes. *Org. Geochem.* **37**, 1477–1488.

Cheng C. H., Lehmann J., Thies J. E. and Burton S. (2008) Stability of black carbon in soils across a climatic gradient. *J. Geophys. Res.* **113**, G02027.

Druffel E. R. M. (2004) Comments on the importance of black carbon in the global carbon cycle. *Mar. Chem.* **92**, 197–200.

Edwards N. T. (1982) The use of soda-lime for measuring respiration rates in terrestrial systems. *Pedobiologia* **23**, 321–330.

Falloon P. D. and Smith P. (2000) Modelling refractory soil organic matter. *Biol. Fert. Soils* **30**, 388–398.

Forbes M. S., Raison R. J. and Skjemstad J. O. (2006) Formation, transformation and transport of black carbon (charcoal) in terrestrial and aquatic ecosystems. *Sci. Total Environ.* **370**, 190–206.

Glaser B. (1999) *Eigenschaften und Stabilität des Humuskörpers der ''Indianerschwarzerden'' Amazoniens*. .

Glaser B., Balashov E., Haumaier L., Guggenberger G. and Zech W. (2000) Black carbon in density fractions of anthropogenic soils of the Brazilian Amazon region. *Org. Geochem.* **31**, 669–678.

Goldberg E. D. (1985) *Black Carbon in the Environment: Properties and Distribution*. John Wiley and Sons, New York.

Grogan P. (1998) CO_2 flux measurement using soda lime: correction for water formed during CO_2 adsorption. *Ecology* **79**, 1467–1468.

Haberstroh P. R., Brandes J. A., Gėlinas Y., Dickens A. F., Wirick S. and Cody G. (2006) Chemical composition of the graphitic black carbon fraction in riverine and marine sediments at submicron scales using carbon X-ray spectromicroscopy. *Geochim. Cosmochim. Acta* **70**, 1483–1494.

Hassink J. (1993) Relationship between the amount and the activity of the microbial biomass in Dutch grassland soils: comparison of the fumigation–incubation method and the substrate-induced respiration method. *Soil Biol. Biochem.* **25**, 533–538.

Jones T. P., Chaloner W. G. and Kuhlbusch T. A. J. (1997) Proposed bio-geological and chemical based terminology for fire-altered plant matter. In *Sediment Records of Biomass Burning and Global Change*, vol. 1 (eds. J. S. Clarks, H. Cachier, J. G. Goldammer and B. J. Stocks). Springer-Verlag, Berlin, pp. 9–22.

Kawamoto K., Ishimaru K. and Imamura Y. (2005) Reactivity of wood charcoal with ozone. *J. Wood Sci.* **51**, 66–72.

Kuhlbusch T. A. J. and Crutzen P. J. (1996) Black carbon, the global carbon cycle and atmospheric carbon dioxide. In *Biomass Burning and Global Change. Chapter 16* (ed. J. S. Levine). The MIT Press, Cambridge, MA, pp. 160–169.

Kuhlbusch T. A. J. (1998) Black carbon and the carbon cycles. *Science* **280**, 1903–1904.

Lehmann J., Liang B. Q., Solomon D., Lerotic M., Luizão F., Kinyangi J., Schäfer T., Wirick S. and Jacobsen C. (2005) Near-edge X-ray absorption fine structure (NEXAFS) spectroscopy for mapping nano-scale distribution of organic carbon forms in soil: application to black carbon particles. *Global Biogeochem. Cycles* **19**, GB1013.

Lerotic M., Jacobsen C., Schäfer T. and Vogt S. (2004) Cluster analysis of soft X-ray spectromicroscopy data. *Ultramicroscopy* **100**, 35–57.

Liang B., Lehmann J., Solomon D., Kinyangi J., Grossman J., O'Neill B., Skjemstad J. O., Thies J., Luizão F. J., Petersen J.

and Neves E. G. () Black carbon increases cation exchange capacity in soils. *Soil Sci. Soc. Am. J.* **70**, 1719–1730.

Masiello C. A. (2004) New directions in black carbon organic geochemistry. *Mar. Chem.* **92**, 201–213.

Müller T. and Höper H. (2004) Soil organic matter turnover as a function of the soil clay content: consequences for model applications. *Soil Biol. Biochem.* **36**, 877–888.

Nelson P. N. and Baldock J. A. (2005) Estimating the molecular composition of a diverse range of natural organic materials from solid-state ^{13}C NMR and elemental analyses. *Biogeochemistry* **72**, 1–34.

Neves E. G., Petersen J. B., Bartone R. N. and Silva C. A. D. (2003) Historical and socio-cultural origins of Amazonian Dark Earths. In *Amazonian Dark Earths: Origin, Properties, Management* (eds. J. Lehmann, D. C. Kern, B. Glaser and W. I. Woods). Kluwer Academic Publishers, Dordrecht, The Netherlands, pp. 29–50.

Nishimiya K., Hata T. and Imamura Y. (1998) Analyses of chemical structure of wood charcoal by X-ray photoelectron spectroscopy. *J. Wood Sci.* **44**, 56–61.

Oades J. M. (1988) The retention of organic matter in soils. *Biogeochemistry* **5**, 35–70.

Pessenda L. C. R., Gouveia S. E. M. and Aravena R. (2001) Radiocarbon dating of total soil organic matter and humin fraction and its comparison with ^{14}C ages of fossil charcoal. *Radiocarbon* **43**, 595–601.

Preston C. M. and Schmidt M. W. I. (2006) Black (pyrogenic) carbon in boreal forests: a synthesis of current knowledge and uncertainties. *Biogeosciences* **3**, 211–271.

Proctor A. and Sherwood P. (1982) XPS studies of carbon fiber surface. *Surf. Interface Anal.* **4**, 213.

Ravel B. and Newville M. (2005) Athena, artemis, hephaestus. *J. Synchrotron Rad.* **12**, 537–541.

Rutherford P. M. and Juma N. G. (1992) Influence of soil texture on protozoa induced mineralisation of bacteria carbon and nitrogen. *Can. J. Soil Sci.* **72**, 183–200.

Schmidt M. W. I. and Noack A. G. (2000) Black carbon in soils and sediments: analysis, distribution, implications, and current challenges. *Global Biogeochem. Cycles* **14**, 777–793.

Schmidt M. W. I. (2004) Carbon budget in the black. *Nature* **42**, 305–306.

Seiler W. and Crutzen P. J. (1980) Estimates of gross and net fluxes of carbon between the biosphere and the atmosphere from biomass burning. *Climatic Change* **2**, 207–247.

Schäfer T., Buckau G., Artinger R., Kim J. I., Geyer S., Wolf M., Bleam W. F., Wirick S. and Jacobsen C. (2005) Origin and mobility of fulvic acids in the Gorleben aquifer system: implications from isotopic data and carbon/sulfur XANES. *Org. Geochem.* **36**, 576–582.

Scheinost A. C., Kretzschmar R., Christl I. and Jacobsen C. (2001) Carbon group chemistry of humic and fulvic acid: a comparison of C-1s NEXAFS and ^{13}C-NMR spectroscopies. In *Humic Substances: Structures, Models and Functions* (eds. E. A. Ghabbour and G. Davies). Royal Society of Chemistry, Cambridge, UK, pp. 39–47.

Schumacher M. (2005) *Microheterogeneity of Soil Organic Matter Investigated by C-1s NEXAFS Spectroscopy and X-ray Microscopy*. Ph.D. Thesis, ETH Zürich.

Schumacher M., Christl I., Scheinost A. C., Jacobsen C. and Kretzschmar R. (2005) Heterogeneity of water-dispersible soil colloids investigated by Scanning Transmission X-ray Microscopy and C-1s XANES microspectroscopy. *Environ. Sci. Technol.* **39**, 9094–9100.

Shindo H. (1991) Elementary composition, humus composition, and decomposition in soil of charred grassland plants. *Soil Sci. Plant Nutr.* **37**, 651–657.

Skjemstad J. O., Clarke P., Taylor J. A., Oades J. M. and McClure S. G. (1996) The chemistry and nature of protected carbon in soil. *Aust. J. Soil Res.* **34**, 251–271.

Skjemstad J. O., Taylor J. A. and Smernik R. J. (1999) Estimation of charcoal (char) in soils. *Commun. Soil Sci. Plant Nutr.* **30**, 2283–2298.

Solomon D., Lehmann J., Kinyangi J., Liang B. and Schäfer T. (2005) Carbon K-edge NEXAFS and FTIR-ATR spectroscopic investigation of organic carbon speciation in soils. *Soil Sci. Soc. Am. J.* **69**, 107–119.

Sohi S. P., Mahieu N., Arah J. R. M., Powlson D. S., Madari B. and Gaunt J. L. (2001) A procedure for isolating soil organic matter fractions suitable for modeling. *Soil Sci. Soc. Am. J.* **65**, 1121–1128.

Stöhr J. (1996) *NEXAFS Spectroscopy*. Springer, Berlin.

Trumbore S. (2000) Age of soil organic matter and soil respiration: radiocarbon constraints on belowground C dynamics. *Ecol. Appl.* **10**, 399–411.

Wang W. J., Dalal R. C., Moody P. W. and Smith C. J. (2003) Relationships of soil respiration to microbial biomass, substrate availability and clay content. *Soil Biol. Biochem.* **35**, 273–284.

Waschkies C. and Hüttl R. F. (1999) Microbial degradation of geogenic organic C and N in mine spoils. *Plant Soil* **213**, 221–230.

Associate editor: Jack J. Middelburg